ENERGYSOLUTIONS

DR - 2012-001220

March 9 2012

CD12 0065

Mr Rusty Lundberg
Executive Secretary
Utah Division of Radiation Control
Utah Division of Water Quality
195 North 1950 West
P O Box 144850
Salt Lake City, UT 84114 4850

RECEIVED
MAR 09 2012
DEPARTMENT OF
ENVIRONMENTAL QUALITY

Re Radioactive Material License #UT 2300249 and Ground Water Quality Discharge Permit No UGW450005 Amendment and Modification Request – Class A West Embankment Revised Well Spacing Analysis

Dear Mr Lundberg

Please find enclosed with this letter a revised well spacing analysis for the Class A West embankment prepared in accordance with a conversation held between Robert Sobocinski (Energy*Solutions*) and Dave Edwards (Division of Radiation Control) on Thursday March 1 Input/output files that support the well spacing analysis have also been provided electronically

Energy*Solutions* will provide a complete electronic file for the entire application when it submits outstanding responses to the seismic and liquefaction work required by the Division

If you have any questions regarding this issue please contact me or Robert Sobocinski at 801 649 2000

Sincerely

Timothy L Orton

for Sean McCandless
Director Compliance and Permitting

enclosures

cc John Hultquist DRC (w/ encl)
Dave Edwards DRC (w/ encl)

I certify under penalty of law that this document and all attachments were prepared under my direction or supervision in accordance with a system designed to assure that qualified personnel properly gather and evaluate the information submitted Based on my inquiry of the person or persons who manage the system, or those persons directly responsible for gathering the information the information submitted is to the best of my knowledge and belief true accurate and complete I am aware that there are significant penalties for submitting false information including the possibility of fine and imprisonment for knowing violations

ENERGYSOLUTIONS

CLIVE FACILITY

WELL SPACING EVALUATION
CLASS A WEST EMBANKMENT

March 9, 2012

For
Utah Division of Radiation Control
195 North 1950 West
Salt Lake City, UT 84114 4850

Energy*Solutions*, LLC
423 West 300 South, Suite 200
Salt Lake City, UT 84101

1 0 INTRODUCTION

Energy*Solutions* proposes to construct the Class A West (CAW) embankment in the northwest quarter of Section 32 at its Clive facility The proposed CAW embankment would encompass the existing Class A and Class A North (CAN) embankments (Figure 1)

This report presents the results of a monitoring well spacing evaluation performed for the CAW embankment A compliance monitoring well network was developed for the CAW embankment The network includes 18 existing wells from the Class A and CAN compliance well networks and also includes 9 proposed new monitoring wells (Figure 1) The monitoring well network is designed to verify regulatory compliance with the State of Utah Ground Water Protection Levels (GWPLs) and to provide early warning of potential releases The spacing of the new wells is consistent with the spacing of the existing wells and also meets the requirement of the Clive facility s Ground Water Quality Discharge Permit (GWQDP) for wells to be located no further than 90 feet from the edge of the waste (Part I F 1 e)

The monitoring well network was evaluated to determine the optimum location for new monitoring wells to detect potential releases with at least 90% efficiency This efficiency criterion was established by the Utah Division of Radiation Control (DRC 2002)

The well spacing evaluation was conducted using the Monitoring Efficiency Model (MEMO) developed by Golder Associates Inc (1992) The MEMO model generates multiple groundwater plumes emanating from a user defined source area and determines whether each potential plume would be detected The efficiency of the monitoring well network is calculated by MEMO as the ratio of the number of plumes that would be detected divided by the total number of potential source releases The objective of the modeling is to design a monitoring network that will detect at least 90% of the potential plumes before they arrive at the boundary The modeling is performed using iodine 129 (I 129) and technetium 99 (Tc 99) as the surrogate contaminants These radionuclides were selected because of their potential presence in CAW embankment Class A waste their conservative transport characteristics (they are relatively mobile) and because of their long half lives relative to the modeled time period of 500 years

This report summarizes the model code documents input parameters and presents results An optimized spacing is presented for the monitoring well network surrounding the proposed CAW embankment Model input/output files are included in Attachment A and well spacing model output is shown graphically in figures in Attachment B This report dated March 9 2012 supersedes the version dated April 28 2011

2 0 MODEL CODE

MEMO is a contaminant transport model that provides a simple computerized method for optimizing monitoring well locations for groundwater monitoring networks at waste management areas MEMO was developed for the U S Department of Energy for evaluation and optimization of the monitoring well network at the Hanford Nuclear Weapons Site near Richland Washington The model incorporates the facility and source geometry site hydrogeology fate and transport characteristics of a specified contaminant and initial monitoring well locations to arrive at a quantified well efficiency value

The efficiency determination is based on whether a plume is detected by the monitoring well network before it crosses a specified buffer zone boundary MEMO identifies areas within a potential contaminant source area where chemical releases would or would not be detected by downgradient monitoring wells Monitoring efficiency is defined as the number of leaks detected compared to the number of non detected leaks For example 90 out of 100 leaks detected at downgradient monitoring well locations would result in a monitoring efficiency of 90%

MEMO incorporates the analytical solution developed by Domenico and Robbins (1985) and Domenico (1987) to predict the configuration of the plume as it migrates downgradient from a continuous source The code is an analytical solution to the advection dispersion partial differential equation of contaminant transport processes in groundwater The model incorporates one dimensional groundwater velocity longitudinal and transverse dispersion the first order degradation rates finite contaminant source dimensions and a steady state source to solve for contaminant concentrations as a function of space and time Additional information on the analytical solution used in MEMO is available in the well spacing evaluations for the Mixed Waste and CAN Embankments performed by Whetstone Associates (Whetstone Associates 2009a and 2009b)

The use of a steady state (continuous) source is a common approach to modeling plume detection A continuous rather than a finite source of leachate assures that releases from leaks near the upgradient end of the waste management area do not disperse to below the detection limit (Golder Associates 1992) As the initial concentration of contaminant in the groundwater at the source increases the downgradient width of the plume also increases The expansion of a given contaminant plume decreases with time and at a critical time the plume will reach steady state conditions and stop growing in size

The calculation of monitoring efficiency assumes that the probability of a release is equally likely at any given location within the source area In reality failure is more likely to occur in specific areas of the cell such as the transition from the top slope to the side slope MEMO

output includes plan view maps showing zones from which plumes would or would not be detected so specific areas of interest can be evaluated

3 0 INPUT PARAMETERS

Input required for the MEMO model includes site geometry dispersion, initial contaminant concentration time and nature of source area

3 1 Site Geometry and Coordinate Data

The coordinates used in the MEMO model are equivalent to the Clive site coordinates (based on a local benchmark at 10 000E 10 000N) Model coordinates are shown in Table 10 and discussed below The footprint of the CAW Embankment and the locations of surrounding monitoring wells (existing and proposed) are shown in Figure 1

3 1 1 Source Area Geometry

Two potential source areas were defined for the MEMO simulations (1) the entire footprint of the CAW embankment (5 8x10^{+6} square feet [ft^2] 133 acres) and (2) the area underlying the top slope of the embankment (4 1x10^{+6} ft^2 95 acres) MEMO simulated individual 1 foot (ft) wide point sources within the potential source areas on a 21 ft grid spacing For the entire footprint the 21 ft source grid spacing resulted in 13 217 individual point sources for the maximum contaminant velocities evaluated in the model For the full top slope footprint the 21 ft source grid spacing resulted in 9 362 individual point sources for maximum contaminant velocities MEMO generated a plume using the Domenico analytical model at each grid point then evaluated whether the plume was detected by the monitoring network Each point source and resulting plume were evaluated separately so a single model run evaluated 13 217 separate plume detections for the entire footprint source or 9 362 separate plume detections for the full top slope source

For the conditions of average contaminant velocity the CAW embankment is sufficiently large that the travel time from upgradient areas of the embankment to monitoring wells is greater than the 500 year compliance period For well spacing analysis of these conditions the source area geometry was adjusted to remove the area of the embankment where point sources did not reach the wells within 500 years The 21 ft point source spacing was maintained however the number of individual point sources was less than those listed above for the entire footprint and top slope Refer to Section 3 4 for addition information on adjustment of the source area geometry

The selection of source area geometry is considered to be conservative because of the extremely narrow (1 ft wide) point source area In general a wider source area will produce a wider plume which is more likely to be detected Also if failure were to occur it would be more likely to occur at several points or along the entire interface between the top slope and side slope resulting in a line source with a larger plume width that is significantly more likely to be detected

3 1 2 Buffer Zone Geometry

The buffer zone geometry is defined by a boundary and a grid spacing along that boundary The buffer zone boundary is defined as the limit to which a plume may extend before it should be detected by a monitoring well Plumes that are detected at the monitoring wells before passing the buffer zone boundary are considered to have been detected The model solves for concentration at each grid point along the buffer zone boundary at a spacing defined by the user A grid spacing that is too coarse could cause plumes to be missed while a grid spacing that is too fine could cause excessive numerical computation or the model might fail to run

In previous MEMO modeling of the Class A and Ile (2) cell at the site (Envirocare 2000 and 2002), the buffer zone boundary was determined to be located 100 ft from the edge of the waste As discussed in previous submittals (Envirocare 2000 and 2002) the MEMO model allows only a single dilution contour to be calculated for each model run while both the method detection limit (MDL) contour and Ground Water Protection Level (GWPL) contour are of interest The MDL contour would provide the earliest indicator of a possible release from the cell, and the GWPL contour indicates the point at which the release would exceed the compliance standard To evaluate both contour intervals simultaneously numerical simulations were run to first determine the time for the GWPL to contact the buffer zone then to determine how much farther the MDL contour would migrate in that time period That migration distance (approximately 90 feet) was added to the buffer zone boundary to represent the location and time at which the MDL is detected at the buffer zone boundary and the modeled constituent meets or exceeds the GWPL at a line located 100 feet from the edge of the waste This approach is consistent with previous MEMO modeling at the facility

The buffer zone grid spacing was set at 40 ft for the CAW embankment MEMO failed to run using a grid spacing finer than 40 ft in combination with the 21 ft source area grid spacing Golder Associates (1992) recommends that the spacing of the buffer array and the spacing of the source grid be "of the same order of magnitude "

3 1 3 Monitoring Well Locations

The CAW embankment monitoring well network includes 18 existing wells from the Class A and CAN networks and also includes 9 proposed new monitoring wells (Figure 1) The locations of the monitoring wells were input into the MEMO model using Clive site coordinates Numerous simulations were run using manual iteration to optimize the new well spacing and to obtain the target efficiency of 90% As discussed in Section 1 the spacing of the new wells is generally consistent with the spacing of the existing wells while meeting requirements listed in the GWQDP The optimized monitoring well coordinates are described in Section 4

3 2 Contaminant Velocity

Groundwater velocity in geologic materials is controlled by hydraulic conductivity hydraulic gradient in the vicinity of the study area and effective porosity of the geologic material Based on Darcy's Law the average groundwater velocity can be calculated using the following equation

$$v = \frac{k * i}{\theta_e}$$

Where

K = Hydraulic conductivity [L/T]
i = Hydraulic gradient [L/L]
θ_e = Effective soil porosity

The transport of contaminants in groundwater may be retarded or slowed by physical processes such as sorption filtration or precipitation The contaminant velocity is given by the following equation

$$v_c = \frac{k * i}{\theta_e R_d}$$

Where

R_d = Constituent retardation factor

Note that when the retardation factor (R_d) equals one the preceding equation describes the aquifer velocity In this case the contaminant is unretarded and travels at the rate of groundwater flow

The hydrogeologic data used in determining hydraulic conductivity gradient effective porosity and retardation are described in Section 3 2 1 through 3 2 4 The calculation of contaminant velocity is given in Section 3 2 5

3 2 1 Hydraulic Conductivity

The hydraulic conductivity used in the model was derived from 83 slug tests conducted in 39 wells surrounding the CAW embankment (Table 1) The wells are completed in hydrostratigraphic Units 2 and 3 The geometric mean hydraulic conductivity of the 39 wells is

1 09x10 ^{3} centimeters per second (cm/sec) (3 10 ft/day) while the arithmetic average is 1 57x10 ^{3} cm/sec (4 46 ft/day)

As shown in Table 2 the upper 90% confidence level of the mean results in hydraulic conductivity values of 1 42x10 ^{3} cm/sec (4 02 ft/day) and 1 93x10 ^{3} cm/sec (5 48 ft/day) for the geometric mean and arithmetic mean respectively

3 2 2 Hydraulic Gradient and Direction

Using monthly groundwater elevation data from November 2009 to November 2010 the hydraulic gradient below the Class A and CAN embankments averaged 5 51x10^{-4} and 5 63x10^{-4} ft/ft respectively, based on freshwater heads (Table 3) The maximum allowable gradient below the Class A and CAN embankments is 1 00x10 ^{3} as specified in the GWQDP Both the average and GWQDP maximum gradients were used in the well spacing evaluation for the CAW embankment

The principal direction of groundwater flow in the shallow aquifer below the proposed CAW embankment is approximately N40°E This groundwater flow direction has been used in recent well spacing analyses for both the CAN and Mixed Waste (MW) embankments (Whetstone Associates 2009a and 2009b) Although the MEMO model allows for changes in flow directions by defining multiple gradient zones within the model domain the hydraulic gradient and flow direction are relatively uniform below the CAW embankment and were entered into the MEMO model as a single gradient zone In addition to the base case (N40°E) gradient zone the sensitivity of the well spacing analysis to flow direction was also evaluated

3 2 Aquifer Porosity

The effective porosity value of 0 29 has been used in previous modeling exercises and is regarded by Utah DEQ as a representative value

3 2 4 Retardation Factor (R)

The retardation factor is constituent specific and can be calculated from the sorption coefficient (K_d) according to the following equation

$$R_d = 1 + \frac{\rho K_d}{\theta_e * C}$$

Where

Rd = Retardation factor
ρ = Soil density (kilograms per cubic meter [kg/m^3])
K_d = Soil water distribution coefficient (liters per kilogram [L/kg])
θ_e = Effective soil porosity
C = Conversion factor (1 000 L/ m^3)

The bulk density of the aquifer materials below the CAW embankment is 1 600 kg/m3 Because the MEMO model evaluation addresses only the saturated zone the bulk density of 1 600 kg/m3 is applicable This bulk density value was used in the well spacing analyses for the CAN and MW embankments (Whetstone Associates 2009a and 2009b)

The K_d values for I 129 (0 12 L/kg) and Tc 99 (0 11 L/kg) are very low indicating that these nuclides are relatively mobile These radionuclides and K_d values were used in the well spacing analyses for the CAN and MW embankments (Whetstone Associates 2009a and 2009b) When K_d values approach zero the resulting retardation factor approaches 1 0 indicating conservative (non retarded) transport in groundwater The calculated retardation factors are shown in Table 4

3 2 5 Contaminant Velocity Calculation

Contaminant velocities were calculated using the hydraulic conductivity hydraulic gradient porosity and retardation coefficients described above The calculated velocities are shown in Table 5

The most conservative well spacing analysis uses contaminant velocities based on the maximum allowable hydraulic gradient and 90% confidence interval above the measured arithmetic mean hydraulic conductivity and results in transport velocities of 0 0114 ft/day for I 129 and 0 0118 ft/day for Tc 99 (Table 5) More representative contaminant velocities are based on the average of the measured hydraulic gradient and the measured geometric mean hydraulic conductivity which results in transport velocities of 0 00362 ft/day for I 129 and 0 00375 ft/day for Tc 99 A higher transport velocity results in less lateral spreading of the plume and a closer optimum well spacing Well spacing analyses are performed using the most conservative higher transport velocities and the more representative average velocities

3 3 Source Term

3 3 1 Width of Line Source

The width of the line source depends on the type of leak and on the amount of lateral spreading in the vadose zone prior to the arrival of the compound at the water table A longer line source would result in a greater probability of plume detection The default width of a line source in the

MEMO model is 20 ft In the simulations of the CAW embankment, the line source width was set at 1 ft The release width of 1 ft is considered to be very conservative because any release from the bottom liner will tend to disperse laterally as it migrates vertically through the vadose zone to the water table

3 3 2 Dispersivity

Dispersion is the physical process of groundwater mixing at the plume boundaries causing the periphery of the plume to be reduced in concentration The Domenico solution in the MEMO model uses longitudinal (a_x) and transverse (a_y) dispersivities to describe the mechanical spreading and mixing caused by dispersion Dispersivity of the aquifer is one of the primary parameters that control the fate and transport of contaminants Dispersivity is commonly considered a scale dependent parameter in contaminant fate and transport modeling with longer flow paths resulting in higher dispersivity (for example see Mallants et al 1998)

Equation 14b of Xu and Eckstein (1995) was used to calculate the longitudinal dispersivity value used in the CAW well spacing analysis This equation is based on a weighted least squares method to assess the relationship between field scale and dispersivity Xu and Eckstein used data reviewed by Gelhar et al (1992) Gelhar et al (1992) classified data obtained by field studies as being of low, intermediate or high reliability Equation 14b of Xu and Eckstein (1995) uses a weighting scheme of 1 2 3 for low intermediate high reliability data respectively The U S Environmental Protection Agency (EPA) includes Xu and Eckstein (1995) Equation 14b as a recommended option for determining longitudinal dispersivity in the BIOCHLOR (EPA, 2000) BIOSCREEN (EPA 1996a) and FOOTPRINT (EPA 2008) models Xu and Eckstein (1995) Equation 14b is also the recommend method of calculating longitudinal dispersivity for the RT3D 3 dimensional reactive transport model (PNNL 2002)

Transverse dispersivity was calculated using the relationship that transverse dispersivity is 10% of longitudinal dispersivity ($a_y = 0\ 1a_x$) This is a commonly used relationship documented in the EPA models cited in the paragraph above Other less conservative estimates of the transverse to longitudinal dispersivity ratio are 0 125 (EPA, 1996b) 0 33 (EPA 1986 and ASTM 1995) and the MEMO model default of 0 143 (IGWMC 1992)

For the MEMO well spacing model of the CAW embankment the longitudinal dispersivity (a_x) was set at 27 2 ft which is obtained from Xu and Eckstein (1995) Equation 14b using a flow path length of 1 291 ft the average distance from the center of the top slope to the line of compliance wells The average distance is calculated as the average of 1) the distance from the center of the top slope to the east line of compliance wells and 2) the distance from the center of the top slope to the north line of compliance wells Transverse dispersivity (a_y) was set at 10% of longitudinal dispersivity or 2 7 ft as shown in Table 6

3 3 3 Diffusion Coefficient

Diffusion is an important mechanism for the transport of solutes through the saturated zone in the absence of significant advective flux (Saripalli et al 2002) Molecular diffusion is mixing caused by random molecular motion due to the thermal kinetic energy of the solute in groundwater Diffusion coefficients of salts and gasses in groundwater typically range from about $4x10^{6}$ to $lx10^{4}$ square centimeters per second (cm^2/sec) (Lerman 1971 Figure 10 8 in Domenico and Schwartz 1990) The diffusion coefficients for I 129 and Tc 99 are shown in Table 7 These values were also used in the well spacing analyses performed for the CAN and MW embankments Derivation of the diffusion coefficients is documented in the reports for the CAN and MW well spacing analyses (Whetstone Associates 2009a and 2009b)

3 3 4 First Order Decay Constant

Radioactive material decays according to first order kinetics The decay constants used in the MEMO modeling for the CAW embankment are consistent with the decay constants calculated for I 129 and Tc 99 in the previous CAN and MW well spacing analyses (Whetstone Associates 2009a and 2009b) Based on isotope half lives of $1\ 57x10^{+7}$ and $2\ 12x10^{+5}$ years for 1 129 and Tc 99 respectively the calculated first order decay constants were $1\ 21x10^{10}$ and $8\ 99x10^{9}$ per day as shown in Table 7

3 3 5 Dilution Contour Values

The dilution concentration contour is defined as the ratio of the detection limit concentration to the source concentration The detection limits for I 129 and Tc 99 are 5 and 10 picoCuries per liter (pCi/L) respectively based on typical minimum detectable activities (MDAs) reported for Clive groundwater samples by the analytical laboratory performing radiological analysis

The source concentrations for I 129 and Tc 99 shown in Table 8 are the time weighted average concentrations at the water table presented in the Class A Combined Disposal Cell Infiltration and Transport Modeling Report (Whetstone Associates 2006) Modeling indicated that concentrations of I 129 and Tc 99 at the water table below the top slope area would be zero for the first 95 – 105 years and would exceed GWPLs at the water table 215 years following cell closure based on environmentally conservative modeling assumptions Modeled concentrations of I 129 and Tc 99 would peak at the water table at 588 and 555 years respectively after closure

Based on MDAs and modeled time weighted average concentrations the dilution concentration contour values used in the CAW well spacing analysis are $1\ 38x10^{6}$ for I 129 and $1\ 00x10^{6}$ for Tc 99 The calculated dilution contour value for Tc 99 is $7\ 32x10^{8}$ (Table 8) which is less than

the lowest dilution concentration contour (1 00x10 ^{6}) allowed in the MEMO model Therefore 1 00x10 ^{6} was used as the dilution concentration contour value for Tc 99

3 4 Advection Time

To select the appropriate advection time input parameter it is important to understand the MEMO model solution methods The MEMO model provides two solution options (1) buffer zone with advection time limit and (2) advection time only The "buffer zone with advection time limit" solution method is the model default in which detections are based on the migration of each plume to a specified limiting distance (the buffer zone boundary) The solution is performed as follows

- The model first generates a source grid within the specified source areas using the user defined source grid spacing (21 feet Section 3 1 1)
- The buffer zone boundary (defined as the limit to which a plume may extend before it should be detected by a monitoring well) is broken into an array of buffer points using the user defined buffer zone spacing (40 feet Section 3 1 2)
- For each point in the source grid a critical time (t_c) is calculated when the plume dilution contour first crosses the buffer zone boundary (i e , the concentration at a buffer zone point exceeds the specified dilution concentration) Each buffer zone point is checked for each plume to ensure the minimum time is calculated
- The concentration at each monitoring well is calculated at time t_c If the concentration at any monitoring well meets or exceeds the specified concentration then the leak has been successfully detected Conversely if the concentration at all monitoring wells is below the specified concentration at time t_c then the plume is assumed to be "non detect" and the area surrounding that point on the source grid is identified as a non detect area
- The process is repeated for all points in the source grid

The dilution contour for plumes in the farthest upgradient portion of the source area may not reach the buffer zone boundary in cases where (1) the plume migrates very slowly or (2) the constituent decays rapidly relative to the plume travel time Plumes that do not reach the buffer zone boundary are considered to be not detected by the model and are not differentiated from "non detect' source areas where the constituent arrives at the buffer zone boundary but is not detected by the monitoring well network

Figure 2 shows an example of non detect zones for the CAW embankment resulting from the first case described above Two options exist to correct for the plumes that never arrive (1) modify the source area to exclude the farthest upgradient areas or (2) increase the advection time

to allow sufficient time for all plumes to reach the buffer zone boundary Note that if the constituent being modeled has a short half life or if the constituent is diluted such that it never arrives at the buffer zone, only the first option will work In that case the source geometry is modified to exclude the farthest upgradient areas from (which source plumes would not arrive at the buffer zone boundary) Note that by excluding these areas from the source no credit is taken for these areas in the monitoring efficiency calculation That is the calculation is based on the remaining (reduced) number of source grid points so that non detects from the remaining source points carry more weight

For the CAW modeling I 129 and Tc 99 have long half lives and would arrive at the buffer zone boundary from anywhere within the source area given a sufficiently long advective transport time However the Utah Division of Water Quality performance based groundwater standard for radiological constituents in Clive facility compliance wells is 500 years Therefore the transport time was set to 500 years (182 500 days), and the first option listed above modification of the source area, was selected to perform sensitivity analysis modeling in cases where the embankment footprint or top slope source area initially included non detect zones (runs using average contaminant velocities)

4 0 WELL SPACING ANALYSIS RESULTS

The MEMO model was run to optimize the CAW well spacing as described in the following sections Sensitivity analyses were performed using a range of contaminant transport velocities and groundwater flow directions The efficiency results of all CAW well spacing runs are summarized in Table 9

4 1 Optimized Well Network

Figure 1 presents the final optimized well spacing for the CAW embankment The network consists of 18 existing Class A and CAN wells and 9 new wells as listed in Table 10 The spacing and location of the new wells are based on the following criteria 1) meet the 90% detection efficiency, 2) each well located no further than 90 feet off the edge of the waste 3) retain the existing spacing to the extent possible and 4) not interfere with the location of existing facilities and features (e g Northwest Corner Pond)

The well spacing was optimized by running the MEMO model numerous times to determine the monitoring well network that produced an efficiency of 90% or greater and that also met the other criteria listed above The CAW embankment can be efficiently monitored with well network shown on Figure 1 The optimal distance between the nine new wells to be added to the network is 388 0 feet along the east edge of the embankment and 350 0 feet along the north edge of the embankment The optimized locations of monitoring wells are listed in Table 10 Note that well GW 142 is located 365 0 feet west of GW 143 The additional 15 feet was necessary to keep GW 142 off the Northwest Corner Pond berm This change was included in the well spacing analysis

The MEMO model output for the entire CAW footprint is shown graphically in Figures 3 and 4 for I 129 (CAWI129a) and Tc 99 (CAWTc99a), respectively The MEMO model output for the top slope source area is shown graphically in Figures 5 and 6 (CAWI129d and CAWTc99d respectively) These results are for simulation of monitoring under the base case conditions of a N40°E (50 degrees in model) groundwater flow direction and highest calculated contaminant velocities Note that even for base case conditions CAWI129a and CAWTc99a small non detect zones are present in the simulations (see Figures 3 and 4) The equivalent simulations with the non detect zones excluded are CAWI129s and CAWTc99s Base case detection efficiencies with non detect zones excluded range from 94 1 to 98 4% meeting the 90% efficiency criterion (Table 9)

4 2 Sensitivity Analysis

A sensitivity analysis was conducted to evaluate the effects of uncertainty in groundwater flow direction and contaminant transport velocity on the CAW well spacing The MEMO model was

run using groundwater flow directions more northerly and more easterly than the N40°E base case flow direction For all modeled flow directions well spacing was evaluated for both a conservative high contaminant velocity and an average velocity condition For each well spacing evaluation performed using the average contaminant velocity MEMO was run twice – first for the entire CAW embankment footprint or top slope source area and second with up gradient non detection zones removed from the source area As discussed in Section 3 4 these zones are removed because contaminant transport time from source to buffer zone boundary exceeds 500 years

Table 9 lists the detection efficiencies of the sensitivity analysis simulations All efficiencies are greater than or equal to 90% indicating that the CAW monitoring well network will meet the 90% criterion if the groundwater flow direction deviates from N40°E as shown or if contaminant transport velocities are slower (less conservative) than base case highest calculated velocities The results of the sensitivity analysis are shown graphically in Attachment B figures

5 0 CONCLUSIONS

A monitoring well network consisting of 18 existing Class A and CAN wells and 9 new wells will provide leak detection with greater than 90% efficiency for the proposed CAW embankment The new wells (GW 142 to GW 150) will be located on the east and north sides of the embankment (Figure 1) The optimal distance between new wells is 388 0 feet along the east edge of the embankment and 350 0 feet along the north edge The location of well GW 142 was adjusted an additional 15 feet west (total distance of 365 0 feet from GW 143) prior to the spacing analysis This will keep GW 142 off the Northwest Corner Pond berm

The optimized well spacing will be protective of human health and the environment and will meet the GWQDP requirements for compliance monitoring wells This optimal well spacing results in monitoring well network efficiencies of 94 1% for I 129 from the entire footprint 94 3% for Tc 99 from the entire footprint 98 2% for I 129 from the top slope source area and 98 4% for Tc 99 from the top slope source area A sensitivity analysis demonstrates that monitoring efficiencies will remain greater than or equal to 90% if the groundwater flow direction varies from that used in the base case model or if contaminant transport velocities are slower than the conservatively high velocities used in the base case

The nine new wells in the optimized well spacing will replace existing monitoring wells along the north and east sides of the CAN embankment Deep aquifer monitoring well GW 139D will require abandonment to construct the CAW embankment, and therefore Energy*Solutions* proposes to install deep aquifer monitoring well GW 148D shown on Figure 1 as its replacement

6 0 REFERENCES

American Society for Testing and Materials (ASTM) 1995 Standard Guide for Risk Based Corrective Action Applied at Petroleum Release Sites ASTM E 1739 95(2010)e1 Philadelphia PA

Domenico P A 1987 An analytical model for multidimensional transport of decaying contaminant species Journal of Hydrology 91 49 58

Domenico P A and Robbins G A 1985 A new method of contaminant plume analysis Ground Water Vol 23(4) 476 485

Domenico Patrick A and Schwartz Franklin W 1990 Physical and Chemical Hydrogeology John Wiley & Sons 824 pp

Envirocare of Utah 2000 Letter from Kenneth Alkema to William J Sinclair regarding Class A Cell Well Spacing Analysis August 22 2000 7 pp plus attachments

Envirocare of Utah 2002 Letter from Daniel B Shrum to William J Sinclair regarding lle (2) Well Spacing Analysis Evaluated with Uranium and Molybdenum September 4 2002 8 pp plus tables and attachments

Gelhar L W Welty C and Rehfeldt K R 1992 A critical review of data on field scale dispersion in aquifers Water Resources Research 28(7) 1955 1974

Golder Associates Inc 1992 MAP – Monitoring Network Design Package Version 1 1 IGWMC – FOS 57 Principal Distributor International Ground Water Modeling Center (IGWMC) Colorado School of Mines Golden CO

International Ground Water Modeling Center (IGWMC) (1992) MAP Monitoring Analysis Package FOS 57 Version 1 1 Colorado School of Mines Boulder CO September 1992

Lerman A 1971 Time to Chemical Steady State in Lakes and Ocean *Adv Chem Ser* vol 106 pp 30 76

Mallants D J Marivoet and G Volckaert (1998) Review of Recent Literature on the Dispersivity Parameter for Saturated and Fractured Porous Media Technical Note 44 Dept W&D SCK CEN Mol Belgium

Pacific Northwest National Laboratory (PNNL) (2002) RT3D – A Modular Computer Code for Simulating Reactive Multi Species Transport in 3 Dimensional Groundwater Systems Version 2 5 (Version 1 0 User s Manual 1997 PNNL 11720) Dispersivity recommendations provided in Frequently Asked Questions available at http //bioprocess pnnl gov/rt3d faq htm#qid30

Saripalli K Prasad Seine R Jeffery Meyer Philip D and McGrail B Peter 2002 Prediction of diffusion coefficients in porous media using tortuosity factor based on interfacial areas Ground Water July 1 2002

U S Environmental Protection Agency (EPA) (2008) FOOTPRINT User s Manual Version 1 0 EPA/600/R 08/058 Center for Subsurface Modeling and Support Ground Water and Ecosystem Restoration Division Ada OK June 2008

U S Environmental Protection Agency (EPA) (2000) BIOCHLOR Natural Attenuation Decision Support System User s Manual Version 1 0 EPA/600/R 00/008 National Risk Management Research Laboratory Office of Research and Development Cincinnati OH January 2000

U S Environmental Protection Agency (EPA) (1996a) BIOSCREEN Natural Attenuation Decision Support System User s Manual Version 1 3 EPA/600/R 96/087 National Risk Management Research Laboratory Office of Research and Development Cincinnati OH August 1996

U S Environmental Protection Agency (EPA) (1996b) Soil Screening Guidance Technical Background Document EPA/540/R 95/128 Office of Solid Waste and Emergency Response July 1996 (see Table 1 of Appendix E)

U S Environmental Protection Agency (EPA) (1986) Background Document for the Ground Water Screening Procedure to Support 40 CFR Part 269 — Land Disposal EPA/530 SW 86 047 January 1986

Utah Division of Radiation Control (DRC) 2002 11e (2) Cell Well Spacing Analysis DRC Request for Information Letter from William J Sinclair to Daniel B Shrum August 8 2002

Whetstone Associates Inc 2006 Class A Combined (CAC) Disposal Cell Infiltration and Transport Modeling Report Prepared for Energy*Solutions* LLC May 2006

Whetstone Associates Inc 2009a Well Spacing Evaluation EnergySolutions Mixed Waste Embankment Prepared for Energy*Solutions* LLC March 9 2009

Whetstone Associates Inc 2009b Well Spacing Evaluation EnergySolutions Class A North Embankment Prepared for Energy*Solutions* LLC March 12 2009

Xu M and Y Eckstein (1995) Use of Weighted Least Squares Method in Evaluation of the Relationship Between Dispersivity and Field Scale Ground Water Vol 33 No 6 pp 905 908

TABLES

Table 1 Hydraulic Conductivity Data from Slug Testing

Well	Cell	Total Depth (ft bgs)	Hydra lic Co ductiv ty (ft/day)	Hyd aulic Cond ctı ty (cm/sec)	A e age Well Hyd l c Cond ctı ty (cm/sec)
GW 25	11 e(2)	33 5	2 316	8 17E 04	1 05E 03
			3 326	1 17E 03	
			3 568	1 26E 03	
			2 557	9 02E 04	
			3 154	1 11E 03	
GW 26	11 e(2)	29 5	0 95	3 35E 04	3 31E 04
			0 92	3 26E 04	
GW 27	11 e(2)	29 5	0 125	4 42E 05	3 49E 05
			0 074	2 60E 05	
			0 098	3 44E 05	
GW 81	Class A	34 0	1 49	5 26E 04	5 23E 04
			1 47	5 19E 04	
GW 82	Class A	34 0	1 82	6 42E 04	5 77E 04
			1 45	5 12E 04	
GW 83	Class A	34 0	8 54	3 01E 03	3 05E 03
			8 76	3 09E 03	
GW 84	Clas A	34 0	10 95	3 86E 03	3 75E 03
			10 3	3 63E 03	
GW 85	Class A	34 0	11 14	3 93E 03	3 94E 03
			11 18	3 94E 03	
GW 86	Class A	34 0	4 8	1 69E 03	1 65E 03
			4 57	1 61E 03	
GW 88	Cla A	38 4	2 66	9 38E 04	9 84E 04
			2 92	1 03E 03	
GW 89	Class A	34 0	1 67	5 89E 04	6 26E 04
			1 88	6 63E 04	
GW 90	Class A	34 0	8 86	3 13E 03	2 94E 03
			7 78	2 74E 03	
GW 91	Class A	34 0	5 73	2 02E 03	1 98E 03
			5 48	1 93E 03	
GW 92	Class A	34 0	2 45	8 64E 04	8 68E 04
			2 47	8 71E 04	
GW 93	Class A	34 0	17 04	6 01E 03	5 96E 03
			16 72	5 90E 03	
GW 94	Class A	34 0	12 73	4 49E 03	4 67E 03
			13 71	4 84E 03	

Table 1 Hydraulic Conductivity Data from Slug Testing

W ll	Cell	T tal D pth (ft bgs)	Hyd a l c Conducti ty (ft/day)	Hydraulic Conducti ty (cm/sec)	A e age Well Hyd aul c Co ducti ty (cm/sec)
GW 95	Class A	29 0	1 04	3 67E 04	3 62E 04
			1 01	3 56E 04	
GW 99	Class A	29 0	0 85	3 00E 04	2 95E 04
			0 82	2 89E 04	
GW 100	Class A	29 0	1 78	6 28E 04	6 44E 04
			1 87	6 60E 04	
GW 101	Class A	34 0	2 36	8 33E 04	7 54E 04
			1 91	6 74E 04	
GW 102	Class A	34 0	2 37	8 36E 04	8 52E 04
			2 46	8 68E 04	
GW 106	CAN	38 5	1 75	6 19E 04	6 07E 04
			1 68	5 94E 04	
GW 107	CAN	38 8	1 41	4 96E 04	5 21E 04
			1 54	5 45E 04	
GW 108	CAN	39 0	1 82	6 41E 04	6 27E 04
			1 74	6 13E 04	
GW 109	CAN	38 5	1 84	6 50E 04	6 27E 04
			1 71	6 04E 04	
GW 110	CAN	38 5	2 27	8 00E 04	7 71E 04
			2 1	7 41E 04	
GW 111	CAN	38 5	5 39	1 90E 03	1 73E 03
			4 39	1 55E 03	
GW 112	CAN	38 5	5 95	2 10E 03	2 20E 03
			6 49	2 29E 03	
GW 113	CAN	38 5	3 12	1 10E 03	1 03E 03
			2 69	9 50E 04	
GW 114	CAN	38 5	3 03	1 07E 03	1 13E 03
			3 37	1 19E 03	
GW 115	CAN	38 5	3 94	1 39E 03	1 42E 03
			4 11	1 45E 03	
GW 116	CAN	38 5	6 72	2 37E 03	2 43E 03
			7 06	2 49E 03	
GW 117	CAN	38 5	5 75	2 03E 03	2 13E 03
			6 32	2 23E 03	
GW 125	CAN	38 0	8 67	3 06E 03	3 17E 03
			9 608	3 39E 03	
			8 689	3 07E 03	

Table 1 Hydraulic Conductivity Data from Slug Testing

Well	Cell	Total Depth (ft bgs)	Hyd aul c Conducti ty (ft/day)	Hydraul c Cond cti ty (cm/se)	Ave age Well Hyd lic Conducti ty (cm/sec)
GW 137	CAN	35 5	4 82	1 70E 03	2 06E 03
			6 86	2 42E 03	
GW 138	CAN	39 0	6 49	2 29E 03	2 25E 03
			6 26	2 21E 03	
GW 139	CAN	38 7	3 97	1 40E 03	1 41E 03
			4 01	1 41E 03	
GW 140	CAN	39 4	2 29	8 08E 04	8 08E 04
			2 29	8 08E 04	
GW 141	CAN	35 5	1 81	6 39E 04	6 44E 04
			1 84	6 49E 04	
				Arithmetic Mean K (cm/s)	1 57E 03
				Mean +90 / Confidence Le el	1 93E 03
				Ge metric Mean K (m/s)	1 09E 03
				Ge metric Mean +90 / Confidence Le el	1 42E 03

Table 2 Descriptive Statistics for Hydraulic Conductivity Test Results

Summ ry Stats (cm/sec)		Summary Stats log(cm/sec)	
Mean	1 57E 03	Mean	2 961
Sta dard Erro	2 14E 04	Sta da d Error	0 066
Med a	1 03E 03	Media	2 989
Mode	6 27E 04	Mode	3 203
Sta dard De at on	1 33E 03	Sta dard De iat on	0 415
Sample Variance	1 78E 06	Sample Variance	0 172
Kurtosis	2 12E+00	K rtos s	3 077
Skew ess	1 49E+00	Skewness	0 993
Range	5 92E 03	R nge	2 232
Minimum	3 49E 05	Min m m	4 458
Ma im m	5 96E 03	Ma imum	2 225
Sum	6 14E 02	S m	115 468
Cou t	39	Count	39
Co f dence Le el (90 0 /)	3 60E 04	Co fide c Le l (90 0 /)	0 112
Mea + 90 / CI	1 93E 03		
Ge M an +90 / CI	1 42E 03		

Table 3 Horizontal Hydraulic Gradient

Date	Class A	Class A North
Nov 09	6 08E 04	5 80E 04
Dec 09	5 45E 04	5 25E 04
Jan 10	5 52E 04	5 37E 04
Feb 10	5 73E 04	5 43E 04
Mar 10	5 81E 04	5 25E 04
Apr 10	5 81E 04	5 58E 04
May 10	5 19E 04	5 62E 04
Jun 10	5 45E 04	5 48E 04
Jul 10	5 55E 04	5 68E 04
Aug 10	5 32E 04	5 67E 04
Sep 10	5 34E 04	5 87E 04
Oct 10	5 23E 04	5 95E 04
Nov 10	5 20E 04	6 23E 04
Average	5 51E 04	5 63E 04
GWQDP Limit	1 00E 03	1 00E 03

Groundwater Quality Discharge Permit (GWQDP) limit from Part 1 H 2(d)

Table 4 Calculated Retardation Factors

Constituent	K_d (L/kg)	ρ (kg/m^3)	θ	R_d
I 129	0 12	1 600	0 29	1 662
Tc 99	0 11	1 600	0 29	1 607

Table 5 Calculated Contaminant Velocities

Constituent	Effective Porosity θ	Hydraulic Gradient i (ft/ft)		Hydraulic Conductivity k (ft/day)		Retardation Factor R_d	Seepage Velocity v (ft/day)	Contaminant Velocity v (ft/day)
I 129	0 29	Permit Maximum	1 00E 03	Arithmetic mean +90% CI	5 48	1 662	1 89E 02	1 14E 02
I 129	0 29	Permit Maximum	1 00E 03	Geometric mean +90% CI	4 02	1 662	1 39E 02	8 33E 03
I 129	0 29	Permit Maximum	1 00E 03	Geometric mean	3 10	1 662	1 07E 02	6 44E 03
I 129	0 29	Average	5 63E 04	Arithmetic mean +90% CI	5 48	1 662	1 06E 02	6 40E 03
I 129	0 29	Average	5 63E 04	Geometric mean +90% CI	4 02	1 662	7 79E 03	4 69E 03
I 129	0 29	Average	5 63E 04	Geometric mean	3 10	1 662	6 02E 03	3 62E 03
Tc 99	0 29	Permit Maximum	1 00E 03	Arithmetic mean +90% CI	5 48	1 607	1 89E 02	1 18E 02
Tc 99	0 29	Permit Maximum	1 00E 03	Geometric mean +90% CI	4 02	1 607	1 39E 02	8 62E 03
Tc 99	0 29	Permit Maximum	1 00E 03	Geometric mean	3 10	1 607	1 07E 02	6 66E 03
Tc 99	0 29	Average	5 63E 04	Arithmetic mean +90% CI	5 48	1 607	1 06E 02	6 62E 03
Tc 99	0 29	Average	5 63E 04	Geometric mean +90% CI	4 02	1 607	7 79E 03	4 85E 03
Tc 99	0 29	Average	5 63E 04	Geometric mean	3 10	1 607	6 02E 03	3 75E 03

CI = Confidence interval

Table 6 Dispersivity Values

Average Longitudinal Transport Distance x (ft)	Longitudinal Dispersivity α (ft)	Transverse Dispersivity α_y (ft)
1 291	27 2	2 7

Table 7 Diffusion Coefficients, Half Lives, and Decay Constants

Constituent	Effective Diffusion Coefficient (ft^2/day)	Half Life $t_{1/2}$ (years)	Decay Constant λ (/day)	Half Live Data Source
I 129	1 19E 03	1 57E+07	1 21E 10	Chart of the Nuclides Knolls Atomic Power Laboratory Naval Reactors DOE Rev 1996
Tc 99	9 03E 04	2 11E+05	8 99E 09	National Nuclear Data Center Brookhaven National Laboratory August 1996

Table 8 Source Concentrations and Derivation of Dilution Contours

	I 129	Tc 99
Time weighted average concentration (C pCi/L)	3 63E+06	1 37E+08
Minimum Detectable Activity (MDA pCi/L)	5	10
Dilution Contour (MDA/C)	1 38E 06	7 32E 08

1 00E 06 is lowest dilution contoured allowed by MEMO model so it was used as the Tc 99 dilution contour

Table 9 Summary of Monitoring Efficiency Modeling for the Class A West Embankment

Model Run	Constituent	Type	Source Area	Flow Direction	Contaminant Velocity (ft/day)	Upgradient Non Arrival Zones	Undetected Leaks	Monitoring Efficiency (/)
CAWI129a	I 129	Base Case	Footprint	N40°E	1 14E 02	Included	855 / 13217	93 5
CAWI129b	I 129	Sensitivity	Footprint	N40°E	3 62E 03	Included	6165 / 13217	53 4
CAWI129c	I 129	Sensitivity	Footprint	N40 E	3 62E 03	Excluded	710 / 7561	90 6
CAWI129d	I 129	Base Case	Top Slope	N40 E	1 14E 02	None	167 / 9362	98 2
CAWI129e	I 129	Sensitivity	Top Slope	N40°E	3 62E 03	Included	4287 / 9362	54 2
CAWI129f	I 129	Sensitivity	Top Slope	N40°E	3 62E 03	Excluded	148 / 5077	97 1
CAWI129g	I 129	Sensitivity	Footprint	N62 E	1 14E 02	None	1322 / 13217	90 0
CAWI129h	I 129	Sensitivity	Footprint	N46 E	3 62E 03	Included	6131 / 13217	53 6
CAWI129i	I 129	Sensitivity	Footprint	N46 E	3 62E 03	Excluded	751 / 7630	90 2
CAWI129j	I 129	Sensitivity	Footprint	N0°E	1 14E 02	None	1243 / 13217	90 6
CAWI129k	I 129	Sensitivity	Footprint	N29°E	3 62E 03	Included	6377 / 13217	51 8
CAWI129L	I 129	Sensitivity	Footprint	N29 E	3 62E 03	Excluded	733 / 7314	90 0
CAWI129m	I 129	Sensitivity	Top Slope	N65°E	1 14E 02	None	917 / 9362	90 2
CAWI129n	I 129	Sensitivity	Top Slope	N58°E	3 62E 03	Included	4516 / 9362	51 8
CAWI129o	I 129	Sensitivity	Top Slope	N58 E	3 62E 03	Excluded	506 / 5127	90 1
CAWI129p	I 129	Sensitivity	Top Slope	N0 E	1 14E 02	None	738 / 9362	92 1
CAWI129q	I 129	Sensitivity	Top Slope	N17°E	3 62E 03	Included	5040 / 9362	46 2
CAWI129r	I 129	Sensitivity	Top Slope	N17°E	3 62E 03	Excluded	453 / 4527	90 0
CAWI129s	I 129	Base Case	Footprint	N40 E	1 14E 02	Excluded	772 / 13121	94 1
CAWTc99a	Tc 99	Base Case	Footprint	N40 E	1 18E 02	Included	771 / 13217	94 2
CAWTc99b	Tc 99	Sensitivity	Footprint	N40 E	3 75E 03	Included	5910 / 13217	55 3
CAWTc99c	Tc 99	Sensitivity	Footprint	N40°E	3 75E 03	Excluded	706 / 7739	90 9
CAWTc99d	Tc 99	Base Case	Top Slope	N40 E	1 18E 02	None	154 / 9362	98 4
CAWTc99e	Tc 99	Sensitivity	Top Slope	N40 E	3 75E 03	Included	4072 / 9362	56 5
CAWTc99f	Tc 99	Sensitivity	Top Slope	N40°E	3 75E 03	Excluded	137 / 5192	97 4
CAWTc99g	Tc 99	Sensitivity	Footprint	N63°E	1 18E 02	None	1324 / 13217	90 0
CAWTc99h	Tc 99	Sensitivity	Footprint	N47°E	3 75E 03	Included	5893 / 13217	55 4
CAWTc99i	Tc 99	Sensitivity	Footprint	N47 E	3 75E 03	Excluded	776 / 7811	90 1
CAWTc99j	Tc 99	Sensitivity	Footprint	N0 E	1 18E 02	None	1168 / 13217	91 2
CAWTc99k	Tc 99	Sensitivity	Footprint	N26°E	3 75E 03	Included	6195 / 13217	53 1
CAWTc99L	Tc 99	Sensitivity	Footprint	N26 E	3 75E 03	Excluded	746 / 7508	90 1
CAWTc99m	Tc 99	Sensitivity	Top Slope	N66 E	1 18E 02	None	897 / 9362	90 4
CAWTc99n	Tc 99	Sensitivity	Top Slope	N59 E	3 75E 03	Included	4305 / 9362	54 0
CAWTc99o	Tc 99	Sensitivity	Top Slope	N59 E	3 75E 03	Excluded	518 / 5362	90 3
CAWTc99p	Tc 99	Sensitivity	Top Slope	N0 E	1 18E 02	None	679 / 9362	92 7
CAWTc99q	Tc 99	Sensitivity	Top Slope	N16 E	3 75E 03	Included	4850 / 9362	48 2
CAWTc99r	Tc 99	Sensitivity	Top Slope	N16 E	3 75E 03	Excluded	460 / 4680	90 2
CAWTc99s	Tc 99	Base Case	Footprint	N40°E	1 18E 02	Excluded	747 / 13193	94 3

Refer to discussion in Sections 3 4 and 4 2

Table 10 Optimized Monitoring Well Network for the Class A West Embankment

Well	Model Well Designation	Clive Coordinates	
		Northing (feet)	Easting (feet)
Existing Wells			
GW 88	10	13 695 79	12 709 21
GW 89	11	13 302 32	12 703 06
GW 90	12	12 910 76	12 697 17
GW 91	13	12 516 05	12 690 76
GW 92	14	12 117 04	12 683 66
GW 25	15	12 137 43	11 817 42
GW 26	16	12 150 89	11 078 35
GW 27	17	12 171 23	10 243 49
GW 93	18	12 127 21	12 295 96
GW 94	19	12 143 73	11 496 85
GW 95	20	12 159 57	10 666 92
GW 99	21	12 565 38	10 250 19
GW 100	22	12 958 43	10 259 09
GW 101	23	13 351 91	10 267 65
GW 102	24	13 746 02	10 276 70
GW 106	25	14 061 30	10 292 39
GW 107	26	14 454 18	10 303 03
GW 108	27	14 800 39	10 312 87
New Wells			
GW 142	1	14 902 99	10 613 15
GW 143	2	14 895 54	10 978 15
GW 144	3	14 888 39	11 328 15
GW 145	4	14 881 24	11 678 15
GW 146	5	14 874 09	12 028 15
GW 147	6	14 866 94	12 378 15
GW 148	7	14 859 79	12 728 15
GW 149	8	14 471 79	12 721 91
GW 150	9	14 083 79	12 715 67

Well designation used in MEMO model runs Attachments A and B

FIGURES

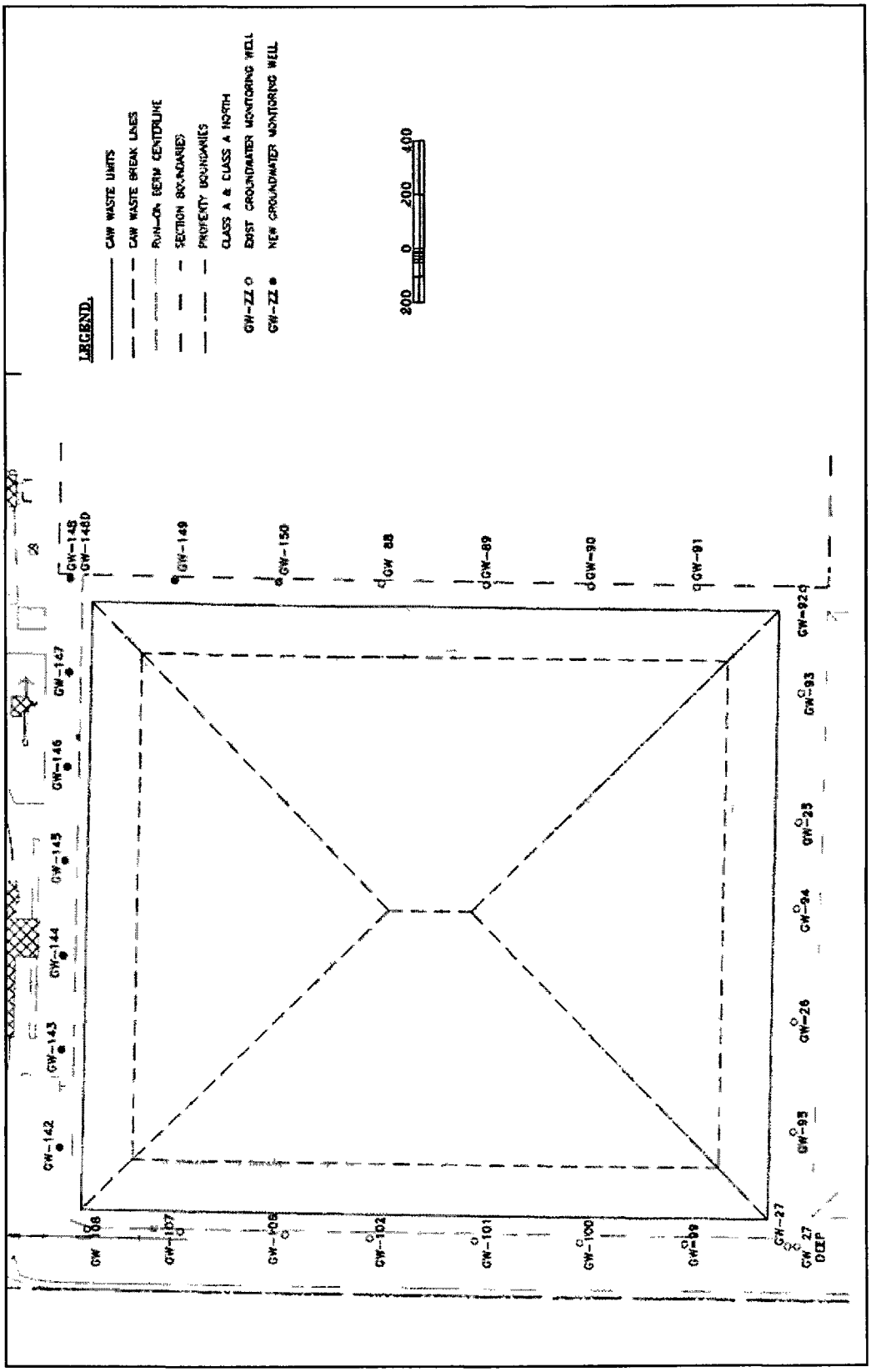

Figure 1 Class A West (CAW) Embankment Optimized Monitoring Well Network with Efficiency Exceeding 95%

Figure 2 Model Results Showing Upgradient Non-Arrival Zone, Model Run CAWI129b, Average Contaminant Velocity, Entire Footprint Source, N40°E Hydraulic Gradient

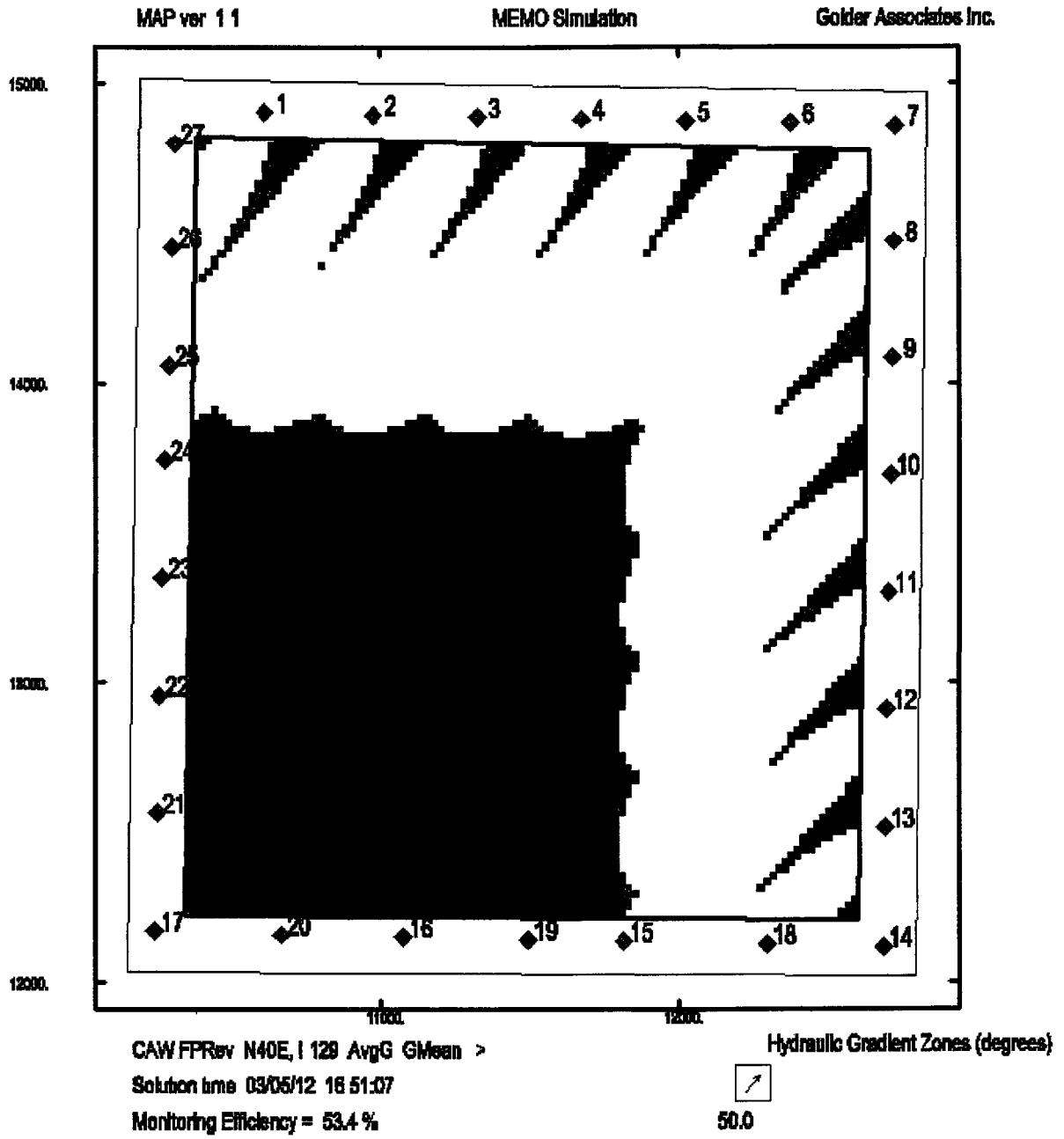

Figure 3 Model Results for I 129, Base Case Conditions, Entire CAW Footprint, Maximum Contaminant Velocity, N40°E Hydraulic Gradient

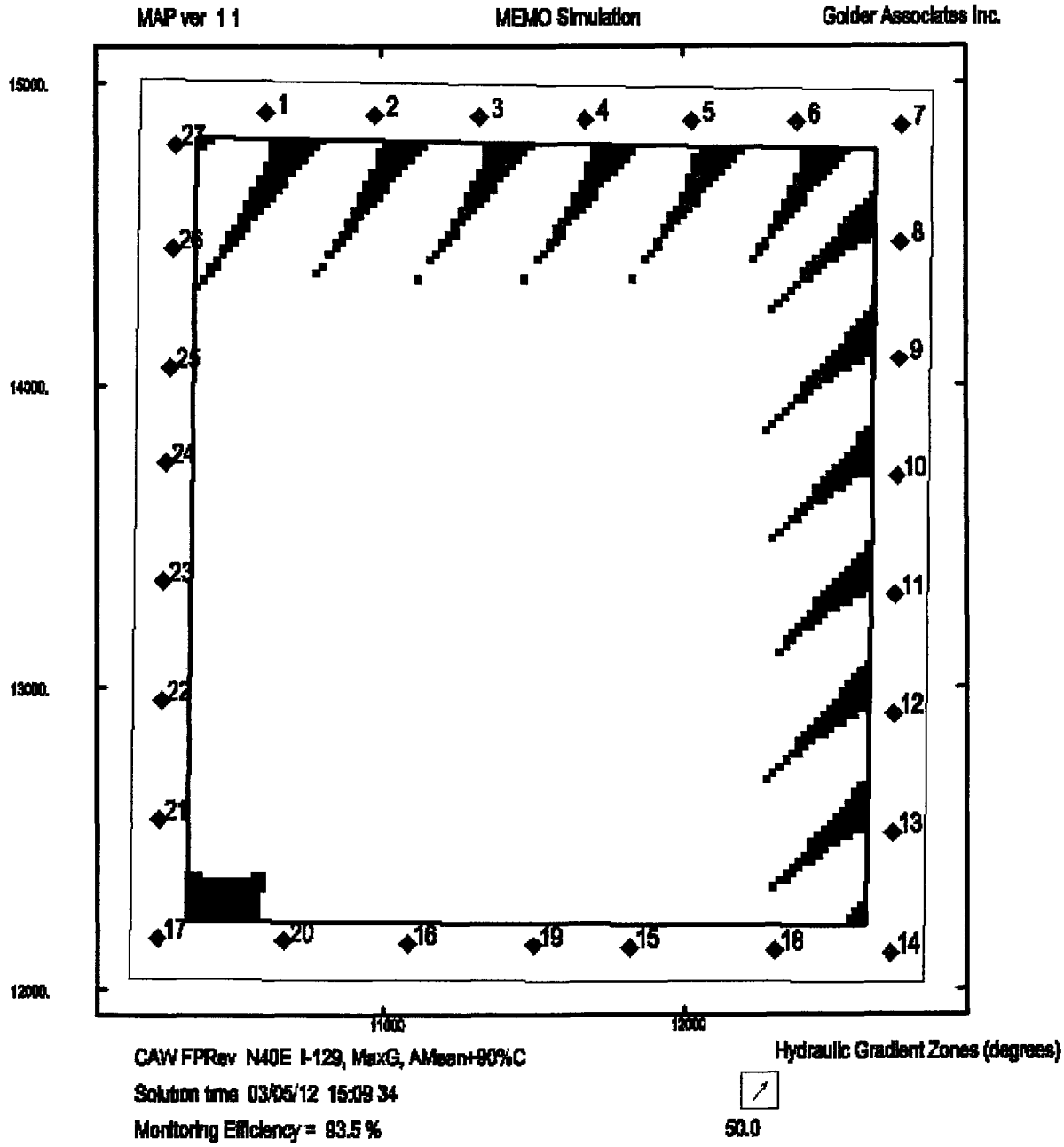

Figure 4 Model Results for Tc 99, Base Case Conditions, Entire CAW Footprint, Maximum Contaminant Velocity, N40°E Hydraulic Gradient

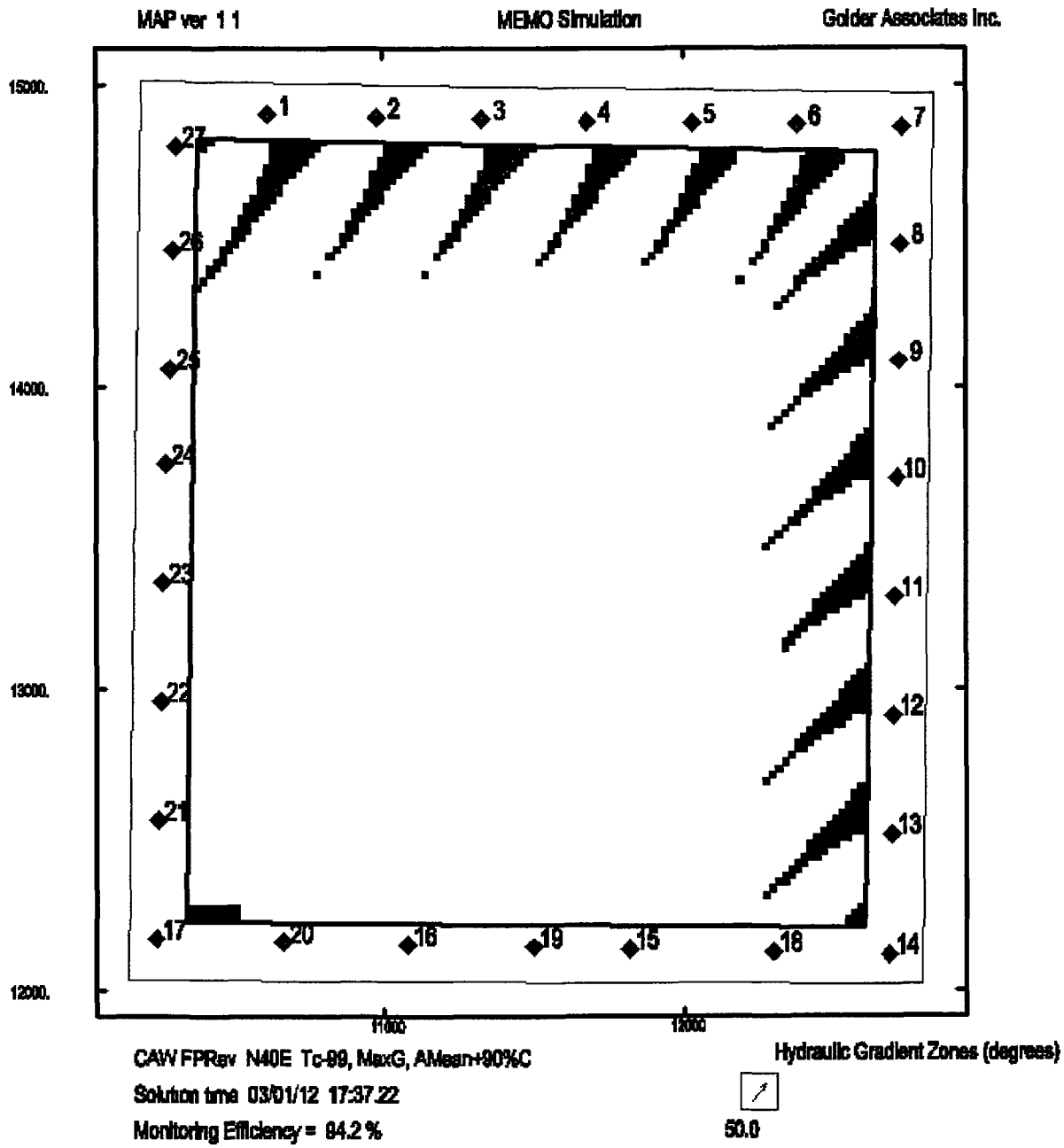

Figure 5 Model Results for I-129, Base Case Conditions, CAW Top Slope, Maximum Contaminant Velocity, N40°E Hydraulic Gradient

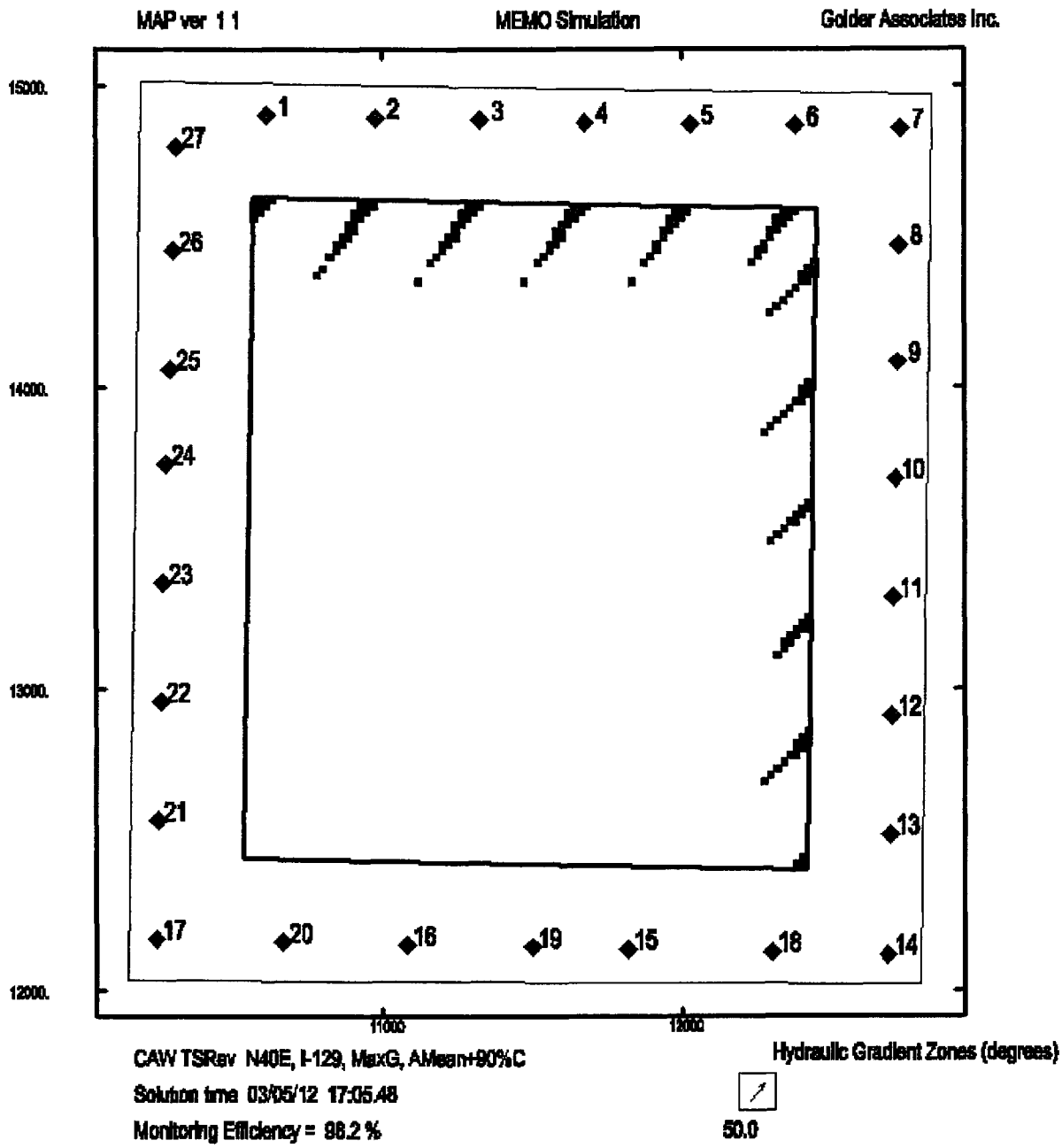

Figure 6 Model Results for Tc 99, Base Case Conditions, CAW Top Slope, Maximum Contaminant Velocity, N40°E Hydraulic Gradient

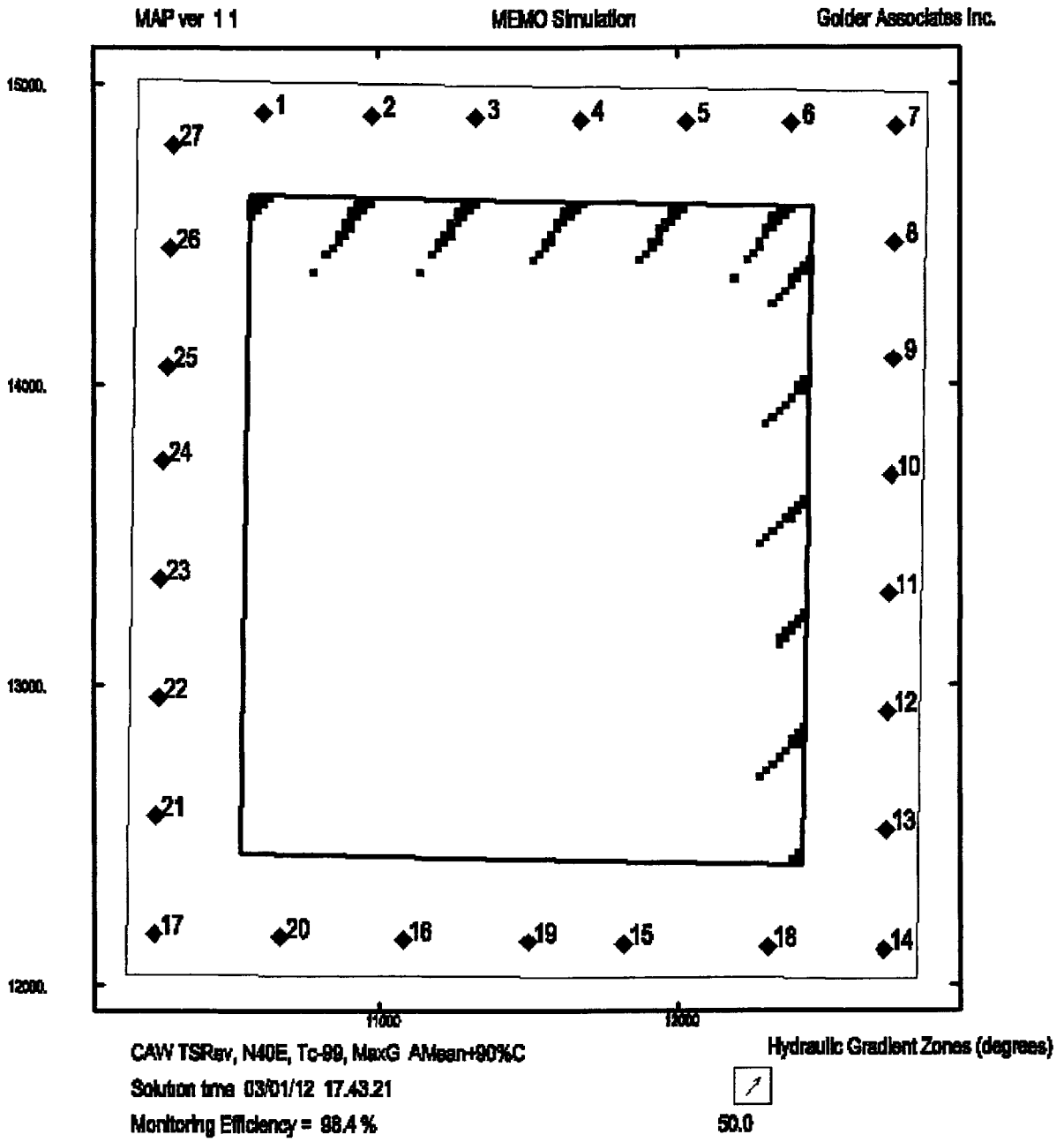

ATTACHMENT A

MEMO MODEL INPUT/OUTPUT FILES

ATTACHMENT B

MEMO MODEL OUTPUT PLOTS